IJSCET

Penerbit UTHM

INTERNATIONAL JOURNAL OF SUSTAINABLE CONSTRUCTION ENGINEERING AND TECHNOLOGY
ISSN: 2180-3242 e-ISSN: 2600-7959

Vol. 17 No. 1 (2026) 260-274
https://publisher.uthm.edu.my/ojs/index.php/ijscet

UAVs-Based Photogrammetric Assessment of Runoff Pathway & Hydrological Surcharge for Drainage Planning

Puteri Izrina Ismi[1], Mohd Fakhrurrazi Ishak[1]*, Solahuddin Daud[1], Zaihasra Abu Talib[2]

[1] *Faculty of Civil Engineering Technology, Universiti Malaysia Pahang Al-Sultan Abdullah, Kuantan, 26300, MALAYSIA*
[2] *Faculty of Civil Engineering and Built Environment, Universiti Tun Hussein Onn Malaysia, Batu Pahat, 86400, MALAYSIA*

*Corresponding Author: fakhrurrazi@umpsa.edu.my
DOI: https://doi.org/10.30880/ijscet.2026.17.01.016

Article Info

Received: 12 June 2025
Accepted: 3 March 2026
Available online: 9 July 2026

Keywords

UAV photogrammetry, surface water runoff, digital elevation model (dem), hydrological surcharge, drainage pathway

Abstract

Urban areas located on steep terrain are prone to surface water accumulation and drainage failures, often causing property damage during heavy rainfall. Jalan Semambu, Beserah, Kuantan, has experienced slope-related issues, including wall cracks, tilted structures, and inadequate drainage, necessitating a detailed assessment of surface runoff and terrain characteristics. This study aims to evaluate slope conditions, surface water behavior, and drainage performance to support effective water-management strategies for the study area. Unmanned Aerial Vehicle (UAV) photogrammetry was employed to capture an aerial image using the Phantom 4 Pro, which Agisoft Metashape processed to generate high-resolution orthophotos and a digital elevation model (DEM). The DEM enabled mapping of five distinct slopes and derivation of quantitative metrics, including slope dimensions, slope area perimeter, and cut-and-fill volumes. Results revealed a consistent runoff pattern where flow from all slopes converges toward a foothill pond, identified as a hydrological surcharge point, and continues downslope toward residential areas, highlighting critical zones of potential flooding. Based on UAV-derived slope gradients, a proposed improved drainage alignment of 55–70 meters was developed to mitigate runoff-related hazards. This study demonstrates that UAV photogrammetry provides an accurate and efficient method for quantifying terrain-controlled runoff, identifying vulnerable areas, and informing practical solutions for a sustainable drainage solution. The findings underscore the potential of UAV-based terrain analysis as a decision-support tool for urban water-management planning in steep-slope residential environments.

1. Introduction

Unmanned aerial vehicles (UAVs), commonly known as drones, have evolved from military applications into powerful tools for civilian geospatial mapping and environmental assessment [1]–[5]. This technology of UAVs, able to acquire high-resolution imagery rapidly and at relatively low cost, has made them valuable for terrain analysis, particularly in areas where traditional survey methods are labour-intensive, time-consuming, or difficult to access [6]-[12]. Conventional ground-based mapping often requires extensive personnel and specialised equipment and poses safety challenges in uneven or vegetated terrain [13], [14].

Digital elevation models (DEMs) and digital orthophoto represent the primary outputs derived from UAV-based photogrammetry [15]. By capturing a series of overlapping aerial photographs, an image produced can be processed in specialised photogrammetric software that applies advanced image-matching algorithms to generate high-resolution DEMs suitable for detailed terrain analysis [7], [16], [17]. In parallel, UAV-based photogrammetry has been increasingly applied in hydrological applications. High-fidelity digital surface models (DSMs) and digital elevation models (DEMs) derived from UAV imagery enable detailed mapping of flow pathways [18], catchment depressions [19], and potential surcharge points [20].

A study conducted by Mazani [18] successfully demonstrated the identification of flow paths in sloped areas through the use of digital elevation models (DEMs) derived from UAV-based mapping. In their study, flow path analysis and catchment delineation were achieved by accurately characterizing the landform, allowing for the determination of natural channels and flow directions governed primarily by gravity. By analysing slope, aspect, and elevation gradients within the DEM, the study was able to predict areas where water is likely to converge, accumulate, or diverge. The study conducted highlights the essential role of DEMs in identifying natural drainage channels, depressions, and potential flood-prone zones, while the inclusion of digital surface models (DSMs) enables consideration of surface features that influence flow patterns, particularly in complex or urbanized terrains.

Another study conducted by Techapinyawat [19] highlighted the use of DEM derived by UAV for identifying catchment areas and flow pathways in urban environments. By capturing detailed terrain information at centimetre-level resolution, the study demonstrated that DEMs can effectively delineate microtopographic features such as small depressions and surface undulations, which control the direction and accumulation of overland flow. The study also noted that UAV-derived DEMs can introduce artificial depressions due to vegetation, temporary objects, or underground infrastructure. The findings of their study suggest the need to quantify the relationships between DEM resolution and associated hydrological attributes and develop new digital drainage analysis algorithms that could effectively incorporate UAV data into urban hydrological modelling.

While the application of UAVs for slope mapping has garnered worldwide attention and application, their use in Malaysia for assessing surface runoff behaviour and drainage-related issues remains limited. Within the Malaysian context, UAV deployment over the past two decades has primarily focused on defence operations [21], coastal monitoring [22], air traffic observation [23], and broad remote-sensing activities [24], leaving hydrological assessments comparatively underexplored. An analysis conducted by Gohari [25] highlighted the number of papers published regarding UAVs and their application in Malaysia from 2018 to 2022. The UAV technology has been applied predominantly in agriculture [26], mapping [27], and forestry [28], with a smaller number of publications focusing on river monitoring, transportation, construction, and coastal management. Only a limited subset of studies has explored the use in flood-related applications [25]. This limitation creates a notable research gap, especially in environments where intense rainfall interacts strongly with modified terrain and inadequate drainage systems. In tropical settings such as Malaysia, frequent high-intensity storms often generate localised surcharge, rapid surface water accumulation, and overflow across sloping ground [29]-[30]. Understanding how runoff traverses these landscapes is therefore critical for safeguarding nearby infrastructure and residential areas.

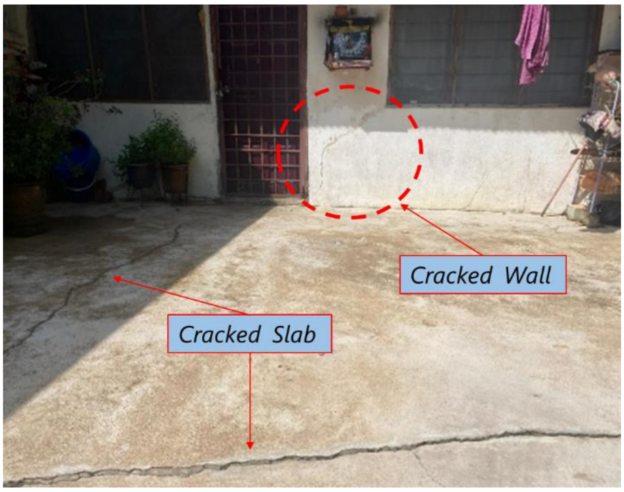

(a)

(b)

(c) (d)

Fig. 1 *Cracks observed around the Semambu residential housing area. (a) Severe cracks on a wall that have been repaired; (b) Cracks around the house porch area; (c) Cracks on the drainage wall opposite the houses; and (d) A house roof exhibiting signs of tilting*

The present study was conducted at Jalan Semambu Beserah, Kuantan, where a natural pond at the foothill accumulates runoff from multiple slopes before overflowing into a nearby housing area. Structural damage to the residential house, as illustrated in Fig. 1, was first observed five months prior to this investigation; rapid deterioration highlighted the need to analyse flow pathways and identify appropriate mitigation measures. UAV photogrammetry was thus employed to generate primary data such as digital orthophotos and digital elevation models (DEMs), enabling detailed mapping of slope characteristics, flow convergence zones, and drainage gaps. The study aims to illustrate how UAV-derived data can be utilized to analyse hydrological surcharge behaviour and inform the design of enhanced drainage solutions for sustainable water management.

2. Methodology

The survey area is at Jalan Semambu-Beserah, Kuantan, Pahang, Malaysia, at an approximate latitude of 3.839262 and longitude of 103.351887. Semambu Residential is situated approximately 3.8 km southwest of Kuantan City and is bordered to the north by Bukit Beserah. The development of this housing area is believed to have commenced in 2003 and predominantly comprises low-cost terraced residences.

This study area was selected as the study site due to its distinctive topographical features and slope conditions, which are highly suitable for this research. The area offers an unobstructed aerial environment, facilitating the free operation of unmanned aerial vehicles (UAVs) without interference. Prior to UAV deployment, it is essential to ensure a clear and safe operational zone, particularly for aerial navigation, as UAVs are vulnerable to disturbances from predatory birds such as eagles and hawks [32]. Fig. 2 illustrates the plan view of the study area.

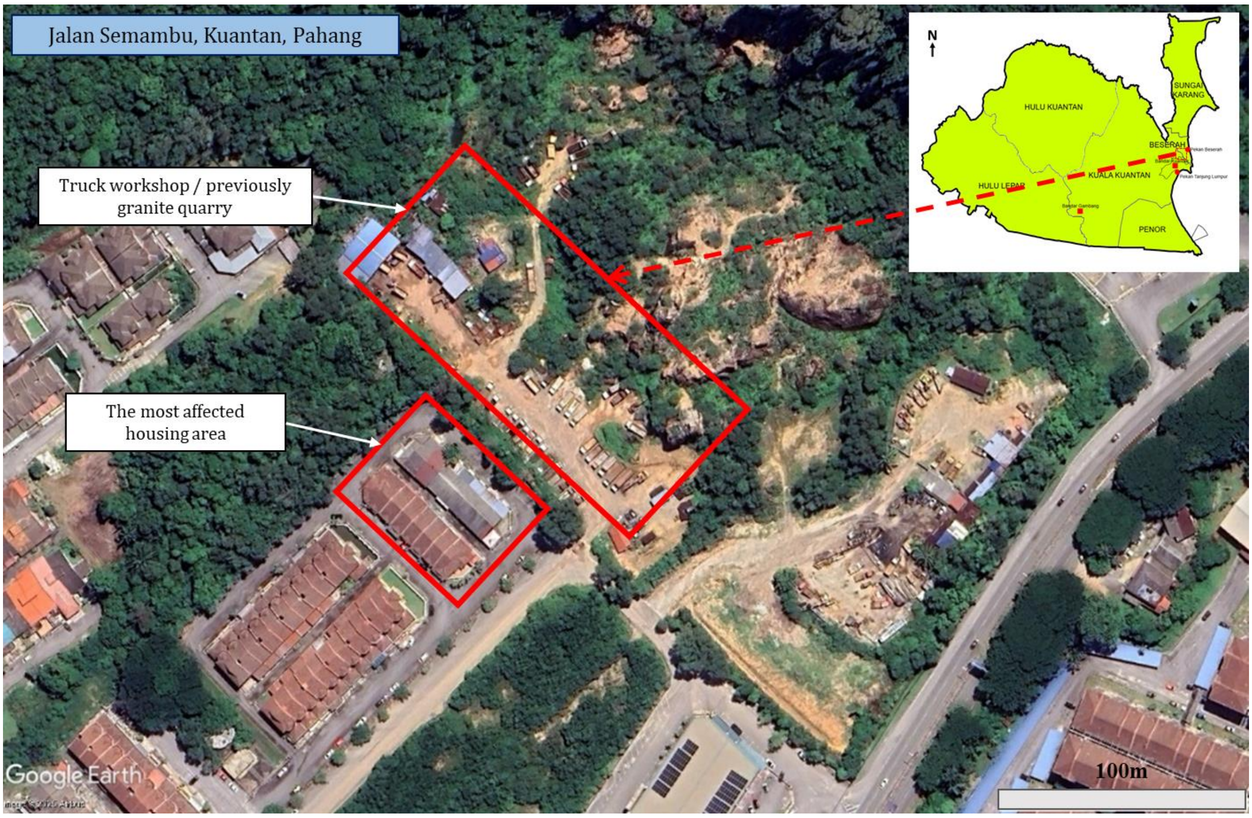

Fig. 2 *Location study*

2.1 UAV Photogrammetric

The study utilised a DJI Phantom 4 Pro, an advanced unmanned aerial vehicle (UAV) engineered for high-resolution aerial mapping and sustainable construction monitoring. It has a total weight of approximately 1.38 kg, inclusive of its battery and propellers, and is capable of achieving a maximum flight speed of 72 km/h in Sport mode. The UAV can ascend at 6 m/s and descend at 4 m/s, providing stable manoeuvrability across varying topographic conditions. With a diagonal dimension of 350 mm (excluding propellers), the Phantom 4 Pro is equipped with a 1-inch, 20-megapixel sensor capable of capturing 4K video at 60 frames per second and 14 frames per second in Burst mode, ensuring exceptional image fidelity for analytical applications. The detailed technical specifications and features of the Phantom 4 Pro are summarised in Table 1 [33], [34].

Table 1 *Specification of DJI Phantom 4 Pro*

Parameter	Details
Weight	1388g
Diagonal size	350mm
Maximum ascent speed	S-mode: 6m/s, P-mode: 5m/s
Maximum descent speed	S-mode:4m/s, P-mode: 3 m/s
Maximum speed	S-mode:45mph, A-mode:36mph, P-mode: 31 mph
Maximum tilt angle	S-mode:42°, A-mode:35°, P-mode: 25°
Maximum angular speed	S-mode: 250°/s, A-mode: 150°/s
Maximum service ceiling above sea level	19685 feet (6000 m)
Maximum flight time per battery	Approximately 30 minutes

On the day of data collection, UAV operations began with system activation, SD card verification, and camera configuration. These field operations are followed by compass calibration and an automatic gimbal check to ensure stable image acquisition. Predefined flight paths were then uploaded, and a brief hover test was conducted prior to the full survey. The setup and calibration procedures required approximately 15 minutes. The UAV subsequently surveyed the entire study area with an effective flight duration of 50 minutes, excluding battery replacement. Overall, the complete data collection process was completed within 1.5 hours, as summarized in Table 2. During the survey, the UAV operated at an altitude of 100 meters with a flight speed of 4 m/s, capturing a total of 171 images for subsequent photogrammetric processing.

Table 2 *UAV flight time estimated*

Component	Duration
Setting Up with Drone Calibration	10 -15 min
Flight Time	50 min
Battery Usage	10 min
Safety Check	5 min
Overall Total	1 hour 30 min

2.2 Image Acquisition and Processing

The standard workflow for UAV image acquisition, as illustrated in Fig. 3, is widely adopted by researchers and UAV practitioners and was applied in this study. The photogrammetry collected by the UAV was processed and stitched using Agisoft Metashape to generate high-resolution orthophotos and a digital elevation model (DEM). These outputs formed the basis for subsequent terrain and hydrological interpretation.

Global Mapper software is used as the primary GIS platform for analysing the UAV-derived datasets [16]. The software provides a versatile environment capable of handling raster, vector, and elevation data, allowing efficient visualisation, editing, and export across multiple formats. Its integrated functions for terrain analysis, profile extraction, spatial measurement, and elevation modelling facilitated a detailed assessment of slope dimensions, cut-and-fill characteristics, and topographic variations across the study area. These tools also supported the extraction of cross-sectional profiles and the interpretation of runoff pathways, enabling a clear understanding of flow convergence patterns and drainage gaps within the site [35].

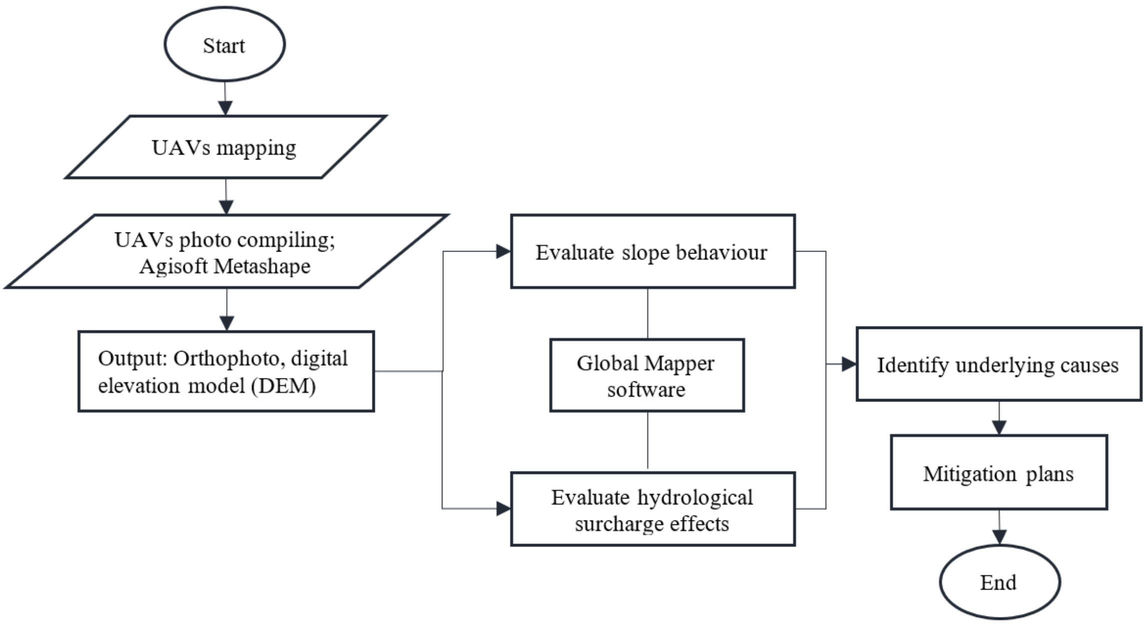

Fig. 3 *Conceptual framework illustrating the methodology applied in this study*

3. Results and Discussion

The outcomes generated throughout each stage of the UAV data acquisition and processing workflow, which includes the production of orthophotos and the digital elevation model (DEM) [36]-[38], as illustrated in Fig. 4, were fundamental to obtaining accurate digital representations of the slope profile. This section presents a detailed analysis of the products derived from UAV-based photogrammetry and their subsequent processing using specialised software. Although ground control points (GCPs) were not employed in this study, the resulting datasets demonstrated minimal positional discrepancy, and the independent orthoimages produced were sufficient for generating reliable digital orthophotos within the photogrammetric workflow.

As noted by Wang [39], the calibration and configuration procedure, which involves both internal camera parameters and external geospatial data, can ensure high-quality outputs suitable for precise 3D modelling and topographic mapping. However, according to Pérez [40], even without GCPs, accuracy can be checked through self-validation within the software by comparing generated models with known secondary reference data or by ensuring that the results are internally consistent.

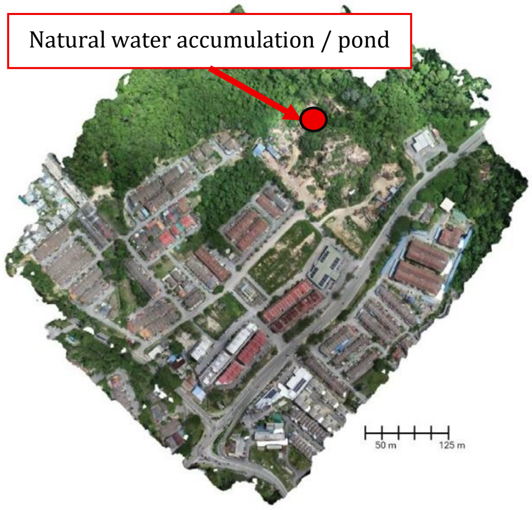

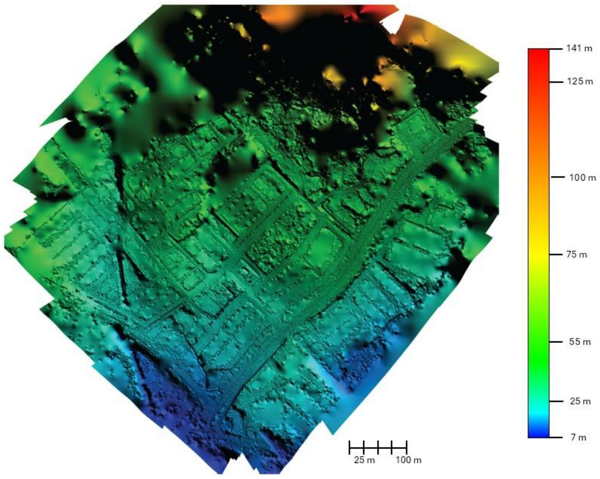

(a) **(b)**

Fig. 4 *(a) Digital orthophoto of the Jalan Semambu–Beserah area, Kuantan; (b) corresponding Digital elevation model (DEM) generated from UAV-based photogrammetry*

3.1 Slope Profile and Dimension

The applications of UAVs extend beyond conventional aerial mapping [41], offering the capability to generate detailed quantitative slope metrics such as perimeter, area, and volumetric estimations [42]. In this study, slope dimensions were derived by using Global Mapper, which enabled the integration of digital orthophotos with the digital elevation model (DEM) to enhance measurement precision. Following the slope measurement, to assess the condition of the slope, the slope angle must be taken into account, as it is one of the key factors contributing to their occurrence [43]. According to Galloway [44], the slope classifications are presented in Table 3. Besides that, Fig. 5 illustrates the spatial distribution of the selected slopes within the study area, while Fig. 6 to 10 present the corresponding area measurements and longitudinal path profiles generated for each slope.

Table 3 *Classification of slope by slope angle. Adapted from Galloway* [44]

Classes of Slope	Angle of slope (°)	Condition of Slope
A	0 – 2	Nearly Level
B	2 – 6	Gently Sloping
C	6 – 12	Moderately Sloping
D	12 – 18	Strongly Sloping
E	18 – 25	Moderately Steep
F	25 – 35	Steep
G	35 -100	Very Steep

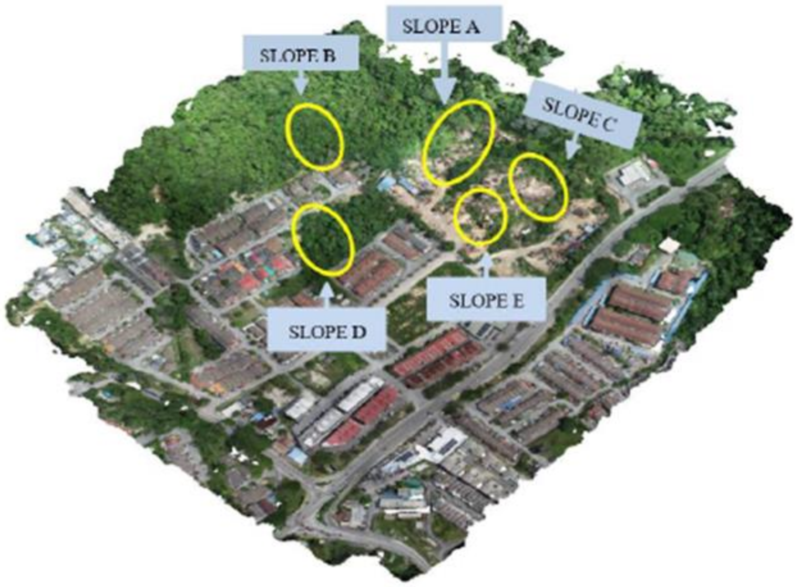

Fig. 5 *Location of the selected slopes within the study area*

Slope A, as depicted in Fig. 6 (a), exhibits the highest total volume at 22,370.56 m^2, accompanied by a net volume of 16,624.81 m^3. The cut and fill analyses indicate a cut volume of 2,872.87 m^3 and a substantially larger fill volume of 19,497.69 m^3. Correspondingly, the cut area is 1,232 m^2, whereas the fill area extends to 4,364 m^2. The measured perimeter of this slope is 312.47 m. Furthermore, the path profile illustrated in Fig. 6(b) demonstrates that the selected section comprises multiple vertices with notable elevation variability. The elevation of the first vertex is approximately 63.233 m, while the second vertex measures 58.201 m, with a horizontal separation of 7.396 m along the x-axis. The calculated slope angle between these two points is 35.04°, which, based on the established slope classification system, categorizes this segment as a *very steep slope*. This classification highlights the high susceptibility of Slope A to slope-related hazards due to its pronounced gradient and significant elevation changes.

(a) **(b)**

Fig. 6 *(a) Area of Slope A; (b) Path profile of Slope A*

As illustrated in Fig. 7(a), Slope B records a total volume of 18,968.76 m^2 and a net volume of 11,523.62 m^3. Notably, it exhibits the highest cut volume among all assessed slopes, measuring 15,246.19 m^3, while the corresponding fill volume is 3,722.57 m^3. The cut and fill areas are 4,129 m^2 and 2,023 m^2, respectively, and the measured perimeter for this slope is 321.92 m. The path profile presented in Fig. 7(b) further indicates that the selected section comprises multiple vertices with distinct elevation differences. The first vertex exhibits an elevation of approximately 34.43 m, whereas the second vertex measures 33.85 m, with a horizontal separation of 5.414 m along the y-axis. The calculated slope angle between these two points is 37.23°, which, according to the established slope classification scheme, classifies this segment as a *very steep slope*. This gradient suggests an elevated susceptibility to slope instability, reinforcing the need for careful geotechnical assessment and mitigation planning in this area.

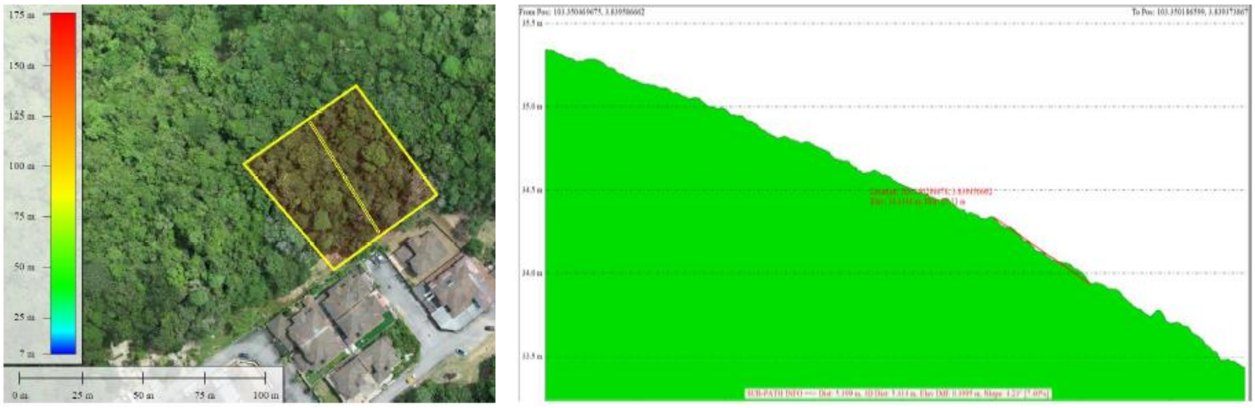

(a) **(b)**

Fig. 7 *(a) Area of Slope B; (b) Path profile of Slope B*

Fig. 8(a) presents the characteristics of Slope C, which records a total volume of 10,683.03 m^2 and the lowest net volume among all slopes at 4,824.06 m^3. The cut volume is measured at 7,753.54 m^3, while the fill volume is comparatively lower at 2,929.48 m^3. The cut area encompasses 1,834 m^2, whereas the fill area is substantially smaller at 141 m^2. The perimeter associated with this slope is 227.85 m. In addition, the path profile illustrated in Fig. 8(b) shows that the selected transect comprises several vertices with pronounced elevation differences. The elevation of the first vertex is approximately 59.75 m, while the second vertex is 48.22 m, with a horizontal separation of 6.993 m along the y-axis. The computed slope angle between these two points is 64.39°, which, according to the established slope classification criteria, categorizes this segment as a *very steep slope*.

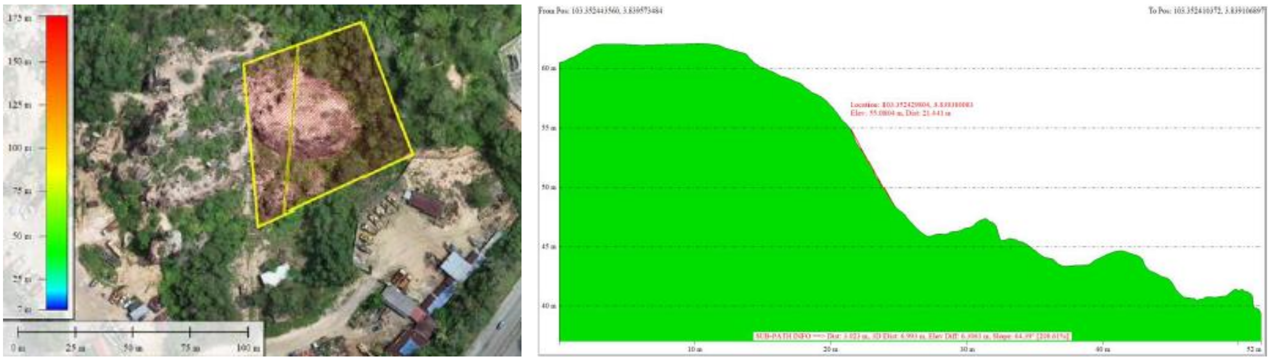

(a) **(b)**

Fig. 8 *(a) Area of Slope C; (b) Path profile of Slope C*

Fig. 9(a) illustrates the characteristics of Slope D, which records a total volume of 15,143.08 m^2 and a net volume of 5,221.30 m^3. The cut volume is measured at 4,960.89 m^3, while the fill volume is substantially higher at 10,182.19 m^3. The cut and fill areas correspond to 1,719 m^2 and 359 m^2, respectively. The perimeter associated with this slope is 305.20 m. The path profile shown in Fig. 9(b) indicates that the selected transect contains several vertices exhibiting slight elevation variations. The elevation of the first vertex is approximately 29.48 m, while that of the second vertex is 29.43 m, with a horizontal separation of 0.583 m along the x-axis. The calculated slope angle between these two vertices is 39.43°, which, according to the established slope classification criteria, categorizes this segment as a *very steep slope*.

(a) **(b)**

Fig. 9 *(a) Area of Slope D; (b) Path profile of Slope D*

Fig. 10(a) presents the characteristics of Slope E, which records a total volume of 11,062.17 m^2 and a net volume of 10,286.07 m^3. The cut volume is measured at 10,674.12 m^3, while the fill volume is the lowest among all slopes at 388.05 m^3. The cut area encompasses 2,219 m^2, whereas the fill area extends to 4,805 m^2. The perimeter associated with this slope is 217.01 m. As shown in Fig. 10(b), the path profile demonstrates that the selected transect consists of several vertices exhibiting notable elevation differences. The elevation of the first vertex is approximately 56.55 m, while the second vertex records an elevation of 50.09 m, with a horizontal separation of 6.46 m along the y-axis. The computed slope angle between these two points is 85.87°, which, based on the established slope classification criteria, classifies this segment as a *very steep slope*. This near-vertical gradient indicates an extremely high susceptibility to slope instability, making Slope E one of the most critical areas requiring detailed geotechnical assessment.

(a) **(b)**

Fig. 10 *(a) Area of Slope E; (b) Path profile of Slope E*

Table 4 presents the dimensional characteristics of each slope, including area, volume, and perimeter, while Table 5 summarizes the corresponding slope classes derived from the calculated horizontal distances and slope angles. Based on the evaluated parameters, all five slopes (Slope A, Slope B, Slope C, Slope D, and Slope E) were classified as *very steep slopes*. This classification aligns with the criteria established under the SOTER model [13], [45], [46], which provides a standardized framework for characterizing slope gradients. The consistent categorization across all slope sections indicates a generally high-gradient terrain, underscoring the potential susceptibility of the study area to slope-related hazards [47].

Table 4 *Summary of dimensional parameters (area, volume, and perimeter) for each slope*

Measurement	Slope A	Slope B	Slope C	Slope D	Slope E
Total volume (m^2)	22370.56	18968.76	10683.03	15143.08	11062.17
Net volume (m^3)	16624.81	11523.62	4824.06	5221.30	10286.07
Cut volume (m^3)	2872.87	15246.19	7753.54	4960.89	10674.12
Cut area (m^2)	1232.00	4129.00	1834.00	1719.00	2219.00
Cut area 3D (m^2)	3286.00	1019.00	3144.00	3671.00	4217.00
Fill volume (m^3)	19497.69	3722.57	2929.48	10182.19	388.05
Fill area (m^2)	4364.00	2023.00	141.00	359.00	4805.00
Fill area 3D (m^2)	823.00	4469.00	2504.00	602.00	670.00
Enclosed area (m^2)	516.00	617.00	3254.00	533.00	2709.00
Perimeter (m)	312.47	321.92	227.85	305.20	217.01

Table 5 *Summary of slope classification categories based on slope angle and horizontal distance*

Slope	Horizontal Distance (m)	Angle of slope (°)	Category	Condition of Slope
A	6.055	35.04	G	Very Steep
B	5.399	37.23	G	Very Steep
C	3.369	64.39	G	Very Steep
D	0.579	39.43	G	Very Steep
E	0.466	85.87	G	Very Steep

The dimensional outputs presented in Table 4, together with the slope classifications summarized in Table 5, provide a clear depiction of the terrain variability within the study area. Variations in slope angle, cut-and-fill volumes, and overall surface geometry are particularly significant for interpreting the interaction between rainfall and the landscape, as these factors govern runoff pathways and influence local flow accumulation patterns. These parameters form the foundation for the subsequent analysis of hydrological surcharge conditions, enabling a more precise assessment of water routing across the slopes and its potential impacts on downstream areas.

3.2 Hydrological Surcharge and Runoff Path Behaviour

The slope dimensions and classifications established earlier provide an essential foundation for examining how surface water is routed across the study area during rainfall events. Variations in slope angle, cut-and-fill geometry, and enclosed areas directly influence the direction and concentration of runoff, shaping the hydrological response during prolonged precipitation. All five slopes examined in the study area (Slopes A, B, C, D, and E) are classified as very steep based on their measured slope angles. Although they fall within the same classification, subtle differences in gradient profiles and elevation transitions still influence their hydrological behaviour. The steeper sections within these slopes promote rapid surface runoff and reduce infiltration potential. In contrast, areas with slightly moderated gradients, though still steep, may temporarily slow water movement or allow brief accumulation in small depressions.

UAV-based photogrammetric and DEM analysis show that runoff from the upper terrain consistently converges toward the foothill, where a small natural pond has formed. This accumulation zone functions as the main surcharge point during high-intensity rainfall, receiving concentrated flow from multiple contributing slopes. Once the pond reaches its capacity, overflow migrates toward the adjacent residential area by following the lowest terrain gradient. Orthophotos and DEM-derived cross-sections clearly illustrate this runoff pathway, highlighting existing depressions and drainage gaps that enable water to bypass current infrastructure and move directly toward the affected housing zone.

Given the way runoff from the upper slopes naturally converges toward the foothill and subsequently travels through the truck workshop area before approaching the nearby housing zone, a more defined drainage pathway becomes essential to manage this flow effectively. The spatial patterns observed through UAV-derived orthophotos and DEM analysis indicate where water can be intercepted and guided, forming the basis for proposing an improved drainage alignment within the site, as discussed in the following section.

Int. J. Sustain. Constr. Eng. Technol. Vol. 17 No. 1 (2026) p. 260-274

3.3 Proposed Drainage Alignment and Flow

One of the key issues identified from the runoff analysis is the absence of a clearly defined drainage route to accommodate the concentrated flow moving through the truck workshop area. Without a dedicated pathway, surface water tends to disperse across the uneven ground, accelerating soil erosion and creating temporary ponding in low-lying sections. Over time, such conditions may contribute to surface deterioration and allow water to migrate toward nearby residential properties. The proposed drainage alignment shown in Fig. 11 aims to intercept this runoff at a strategic point before it spreads downslope.

To ensure smooth and continuous water conveyance, selected sections of the ground require minor reshaping to achieve a consistent gradient along the intended drainage line. The front contour view and path profile illustrated in Fig. 12(a) and 12(b) highlight the natural elevation drop that can be utilised to guide water efficiently toward a stable outlet. Adjusting these sections helps minimise ponding, reduce sediment deposition, and maintain the direction of flow during high-intensity rainfall.

Proper grading of the proposed drainage channel also plays an important role in reducing the amount of water accumulating around structures within the workshop area. By establishing a defined and continuous flow route, the system helps regulate surface water movement, manage runoff more effectively, and reduce the potential for water encroachment toward the residential zone. Overall, the proposed drainage alignment provides a practical and terrain-responsive solution supported by evidence from UAV-based mapping and analysis.

Fig. 11 *Proposed drainage flow alignment based on UAV-derived terrain analysis*

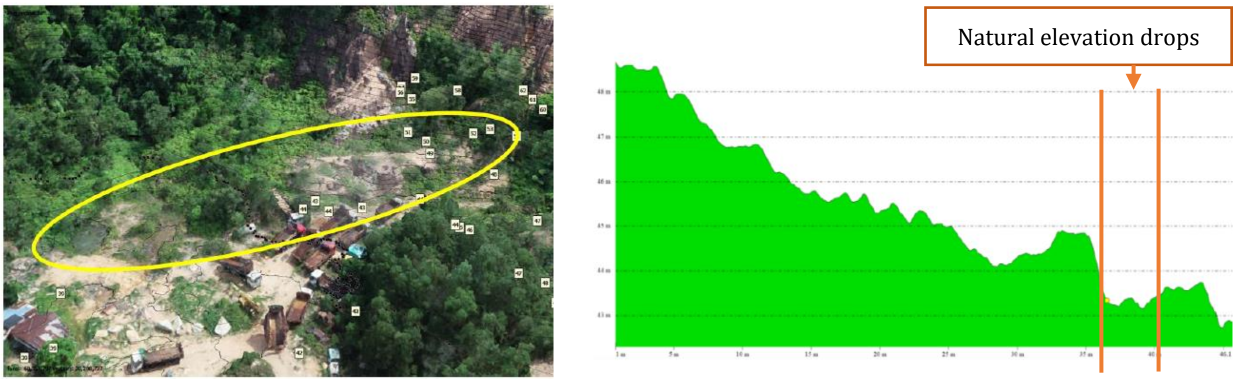

(a) **(b)**

Fig. 12 *(a) Front-view contour representation; (b) Elevation path profile of the proposed drainage alignment*

4. Conclusion

This study demonstrated the application of UAV photogrammetry in characterising surface water behaviour and drainage conditions at Jalan Semambu Beserah through the generation of high-resolution orthophotos and Digital Elevation Models (DEMs). The quantitative outputs, particularly the slope dimensions, cut and fill volumes, and elevation profiles extracted from five slopes, enabled a clear identification of runoff convergence zones. The analysis showed that water from the upper terrain consistently flows toward the foothill, where a natural pond functions as a primary surcharge point before directing overflow toward the nearby residential area. These findings supported the delineation of a proposed drainage alignment, designed to intercept concentrated runoff and guided by terrain indicators captured through UAV-derived data. UAV data acquisition is sensitive to weather conditions; heavy clouds, wind, and intermittent rain can affect image clarity and flight stability. The absence of ground control points (GCPs) reduces the positional accuracy of the DEM [12]; these limits precise elevation referencing and micro-topographic interpretation. The resolution of the photogrammetric outputs also presents constraints, particularly in shaded or vegetated areas; consequently, some fine terrain features may not be fully represented. These limitations indicate the need for additional control measures and ground validation in future studies.

Future work can be enhanced by integrating GIS-based hydrological modelling to simulate flow behaviour under various rainfall scenarios; incorporating ground-based verification methods such as GNSS surveys and water-level measurements; and applying the UAV mapping approach to different terrain conditions to examine its broader applicability. Improvements such as the use of RTK-enabled UAV systems or automated flow-path extraction tools may also strengthen data precision and processing efficiency.

Overall, this study illustrates that UAV photogrammetry is an effective approach for understanding drainage behaviour and proposing practical water-management solutions. By providing rapid, accurate, and high-resolution terrain insights in an area with limited accessibility, the method offers a robust foundation for drainage planning, contributing meaningfully to sustainable and informed infrastructure management in Malaysia.

Acknowledgement

The authors would like to express their gratitude to Universiti Malaysia Pahang Al-Sultan Abdullah (UMPSA) for Grant (RDU243007 – Geran Unggul & RDU252401/UIC250802 – Geran Padanan Industri) that served as full financial support to conduct this research. The authors wish to express their sincere gratitude to the anonymous reviewer for their comprehensive and discerning critique. Their constructive observations have made a significant contribution to strengthening the precision and scholarly rigor of this manuscript.

Conflict of Interest

The authors declare no competing interest.

Author Contribution

*The authors confirm contribution to the paper as follows: **study conception and design**: M F Ishak, P I Ismi; data collection: S Daud; **analysis and interpretation of results**: P I Ismi, S Daud; **draft manuscript preparation**: P I Ismi, M F Ishak, S Daud. All authors reviewed the results and approved the final version of the manuscript.*

References

[1] Adu-Gyamfi, S., Gyasi, R., & Darkwa, B. (2021). Historicizing medical drones in Africa: A focus on Ghana. *History of Science and Technology, 11*, 103–124. https://doi.org/10.32703/2415-7422-2021-11-1-103-125

[2] Elish, M. C. (2017). Remote Split: A History of US Drone Operations and the Distributed Labor of War. *Science, Technology, & Human Values, 46(6)*, 1100–1131. https://doi.org/10.1177/0162243917731523

[3] González, R. J. (2024). Death by remote control: drone warfare in Afghanistan, Ukraine and beyond. *Anthropology Today, 40(1)*, 7–11. https://doi.org/10.1111/1467-8322.12862

[4] Steen, R., Håheim‐Saers, N., & Aukland, G. (2023). Military unmanned aerial vehicle operations through the lens of a high‐reliability system: challenges and opportunities. *Risk, Hazards, & Crisis in Public Policy, 15(3)*, 347‐373. https://doi.org/10.1002/rhc3.12279

[5] Ishak, M. F., Zolkepli, M. F., Daud, S., Yunus, N. Z. M., & Rashid, A. S. A. (2023). The Application of Unmanned Aerial Vehicle (UAV) for Slope Mapping at Gambang Damai Residents, Pahang: A Case Study. *International Journal of Integrated Engineering, 15(2)*, 219–227. https://doi.org/https://doi.org/10.30880/ijie.2023.15.02.021

[6] Su, S., Li, Y., Xie, H., Chen, C., Zhang, X., Gao, L., & Zhang, R. (2024). Multi-level hazard detection using a UAV-mounted multi-sensor for levee inspection. *Drones, 8(3)*, 90. https://doi.org/10.3390/drones8030090

[7] Daud, S., Zolkepli, M. F., Ishak, M. F., & Talib, Z. A. (2024). Suction Variation of a Single Mature Tree on Top of Tropical Residual Soil. *International Journal of Integrated Engineering, 16(9)*, 37–52. https://doi.org/10.30880/ijie.2024.16.09.003

[8] Zolkepli, Muhammad Farhan, Ishak, M. F., Zolfan, F. N. A., Yusoff, N. S., Daud, S., & Zin, N. S. M. (2023). Implementation of Unmanned Aerial Vehicle (UAV) for Slope Mapping. *International Journal of Engineering Technology and Sciences, 10(1)*, 16–23. https://doi.org/10.15282/ijets.10.1.2023.1003

[9] Zolkepli, M. F., Ishak, M. F., & Zaini, M. S. I. (2019). Slope stability analysis using modified Fellenius's and Bishop's method. *IOP Conference Series: Materials Science and Engineering, 527(1)*, 0–12. https://doi.org/10.1088/1757-899X/527/1/012004

[10] Zolkepli, M. F., Ishak, M. F., & Zaini, M. S. I. (2018). Analysis of slope stability on tropical residual soil. *International Journal of Civil Engineering and Technology, 9(2)*, 402–416.

[11] Ishak, M. F., Zolkepli, M. F., Daud, S., Zin, N. S. Z., & Talhah, M. F. M. (2023). Exploration of Secondary Deposit to Determine Manganese Ore Body. *International Journal of Engineering Technology and Sciences, 10(1)*, 24–33. https://doi.org/10.15282/ijets.10.1.2023.1004

[12] Gond, A. K., Ohri, A., Gaur, S., & Das, N. (2025). Accuracy assessment and optimization of the photogrammetric process variable for 3D mapping using unmanned aerial vehicle (drone). *Journal of the Indian Society of Remote Sensing, 53*, 3141 – 3164. https://doi.org/10.1007/s12524-025-02126-x

[13] Zolkepli, M. F., Ishak, M., & Talib, Z. A. (2022). Unmanned aerial vehicle (UAV)-based for slope mapping and the determination of potential slope hazard. *International Journal of Integrated Engineering, 14(1)*. https://doi.org/10.30880/ijie.2022.14.01.021

[14] Daud, S., Ishak, M. F., Ismi, P. I., & Zolkepli, M. F. (2025). Investigation of potential groundwater sources using electrical resistivity imaging for industrial facilities in Gebeng, Kuantan, Malaysia: A case study. *Warta Geologi, 51(2)*, 77–85. https://doi.org/10.7186/wg512202502

[15] Ismail, M. A. M., Kumar, N. S., Abidin, M. H. Z., & Madun, A. (2018). Systemic Approach to Elevation Data Acquisition for Geophysical Survey Alignments in Hilly Terrains Using UAVs. *Journal of Physics: Conference Series, 995(1)*. https://doi.org/10.1088/1742-6596/995/1/012104

[16] Arif, F., Abdul Maulud, K. N., & Ab Rahman, A. A. (2018). Generation of digital elevation model through aerial technique. *IOP Conference Series: Earth and Environmental Science, 169(1)*. https://doi.org/10.1088/1755-1315/169/1/012093

[17] Coveney, S., & Roberts, K. (2017). Lightweight UAV digital elevation models and orthoimagery for environmental applications: data accuracy evaluation and potential for river flood risk modelling. *International Journal of Remote Sensing, 38(8–10)*, 3159–3180. https://doi.org/10.1080/01431161.2017.1292074

[18] Mazani, M. M., Nasir, A. A. M., Rahzaman, N. N. N., & Kaamin, M. (2024). Pemeriksaan Cerun Secara Visual di Bukit Putus,Negeri Sembilan Menggunakan Kaedah Fotogrametri. *Multidisciplinary Applied Research and Innovation, 5(1)*, 102–109. https://doi.org/10.30880/mari.2024.05.01.016

[19] Techapinyawat, L., Goulden-Brady, I., Garcia, H., & Zhang, H. (2023). Aerial characterization of surface depressions in urban watersheds. *Journal of Hydrology, 625*, 129954. https://doi.org/https://doi.org/10.1016/j.jhydrol.2023.129954

[20] Leitão, J. P., Moy De Vitry, M., Scheidegger, A., & Rieckermann, J. (2016). Assessing the quality of digital elevation models obtained from mini unmanned aerial vehicles for overland flow modelling in urban areas. *Hydrology and Earth System Sciences, 20(4)*, 1637–1653. https://doi.org/10.5194/hess-20-1637-2016

[21] Konert, A., & Balcerzak, T. (2022). Military autonomous drones (UAVs) - From fantasy to reality. Legal and Ethical implications. *Transportation Research Procedia, 59*, 292–299. https://doi.org/10.1016/j.trpro.2021.11.121

[22] Darwin, N., Ahmad, A., & Zainon, O. (2014). The potential of unmanned aerial vehicle for large scale mapping of coastal area. *IOP Conference Series: Earth and Environmental Science, 18(1)*. https://doi.org/10.1088/1755-1315/18/1/012031

[23] Congress, S. S. C., Puppala, A. J., Banerjee, A., & Patil, U. D. (2021). Identifying hazardous obstructions within an intersection using unmanned aerial data analysis. *International Journal of Transportation Science and Technology, 10(1)*, 34–48. https://doi.org/10.1016/j.ijtst.2020.05.004

[24] Kaamin, M., Mazuki, M. S., Madun, A., Idris, N., Razak, S. N. A., Ngadiman, N., & Nor, A. H. M. (2020). Visual slope inspection using unmanned aerial vehicle (UAV). *Journal of Physics: Conference Series, 1526*, 1–11. https://doi.org/10.1088/1742-6596/1529/3/032102

[25] Gohari, A., Ahmad, A., & Oloruntobi, O. O. (2023). Recent Drone Applications in Malaysia: an Overview. *International Archives of the Photogrammetry, Remote Sensing and Spatial Information Sciences - ISPRS Archives, 48(4/W6-2022)*, 131–137. https://doi.org/10.5194/isprs-archives-XLVIII-4-W6-2022-131-2023

[26] Istiak, M. A., Syeed, M. M. M., Hossain, M. S., Uddin, M. F., Hasan, M., Khan, R. H., & Azad, N. S. (2023). Adoption of Unmanned Aerial Vehicle (UAV) imagery in agricultural management: A systematic literature review. *Ecological Informatics, 78*, 102305. https://doi.org/https://doi.org/10.1016/j.ecoinf.2023.102305

[27] Liu, Y., Zheng, X., Ai, G., Zhang, Y., & Zuo, Y. (2018). Generating a high-precision true digital orthophoto map based on UAV images. *Canadian Historical Review, 7(9)*. https://doi.org/10.3390/ijgi7090333

[28] Kamarulzaman, A. M. M., Jaafar, W. S. W. M., Said, M. N. M., Saad, S. N. M., & Mohan, M. (2023). UAV Implementations in Urban Planning and Related Sectors of Rapidly Developing Nations: A Review and Future Perspectives for Malaysia. *Remote Sensing, 15(11)*. https://doi.org/10.3390/rs15112845

[29] Sidek, L. M., Jaafar, A. S., Majid, W. H. A. W. A., Basri, H., Marufuzzaman, M., Fared, M. M., & Wei, C. M. (2021). High – resolution hydrological – hydraulic modelling of urban floods using InfoWorks ICM. *Sustainability (Switzerland), 13*, 1–20. https://doi.org/doi.org/10.3390/su131810259

[30] Jelani, J., Suif, Z., Ahmad, N., Rabbani, M. J. R. M. S., & Khairulazman, N. A. (2025). Experimental study of rainfall intensity on silty sand slope. *Sinergi, 29(2)*, 547–554. https://doi.org/10.22441/sinergi.2025.2.024

[31] Daud, S., Ishak, M. F., Ismi, P. I., Muhammad, N., & Ghazali, S. (2025). Granite exploration by using resistivity and induced polarization imaging in western granite belt, Pendang, Kedah, Malaysia. *Smart Construction and Sustainable Cities, 3(23)*. https://doi.org/10.1007/s44268-025-00067-5

[32] Ishak, M., Zolkepli, M., Daud, S., Yunus, N., & Rashid, A. (2022). Unmanned aerial vehicle (UAV) for slope mapping at Perumahan Gambang Damai, Pahang: a case study. *In IET Conference Proceedings (Vol. 2022)*. https://doi.org/10.1049/icp.2022.2677

[33] Taddia, Y., González-García, L., Zambello, E., & Pellegrinelli, A. (2020). Quality assessment of photogrammetric models for façade and building reconstruction using DJI Phantom 4 RTK. *Remote Sensing, 12(19)*, 3144. https://doi.org/10.3390/rs12193144

[34] Peppa, M. V., Hall, J., Goodyear, J., & Mills, J. P. (2019). Photogrammetric assessment and comparison of dji phantom 4 pro and phantom 4 rtk small unmanned aircraft systems. *International Archives of the Photogrammetry, Remote Sensing and Spatial Information Sciences - ISPRS Archives, 42(2/W13)*, 503–509. https://doi.org/10.5194/isprs-archives-XLII-2-W13-503-2019

[35] Ngadiman, N., Badrulhissham, I. A., Mohamad, M., Azhari, N., Kaamin, M., & Hamid, N. B. (2019). Monitoring slope condition using UAV technology. *Civil Engineering and Architecture, 7(6)*, 1–6. https://doi.org/10.13189/cea.2019.071401

[36] Ibrahim, N. A. S. (2020). *Collecting Orthophotos Data for Slope Reconnaissance Using UAV Method*. Universiti Malaysia Pahang (UMP).

[37] Tung, W. Y., Nagendran, S. K., & Ismail, M. A. M. (2018). 3D rock slope data acquisition by photogrammetry approach and extraction of geological planes using FACET plugin in CloudCompare. *IOP Conference Series: Earth and Environmental Science, 169(1)*, 012051.

[38] Jaafar, S. A. N. (2020). *Identification of Slope Hazard from Profile using Unmanned Aerial Vehicle (UAV)*. Universiti Malaysia Pahang (UMP).

[39] Wang, Z., Shi, L., Li, J., Dai, W., Lu, W., & Li, M. (2025). The Synergistic Effects of GCPs and Camera Calibration Models on UAV-SfM Photogrammetry. *Drones, 9(5)*. https://doi.org/10.3390/drones9050343

[40] Pérez, M., Agüera, F., & Carvajal, F. (2012). Digital Camera Calibration Using Images Taken from an Unmanned Aerial Vehicle. *The International Archives of the Photogrammetry, Remote Sensing and Spatial Information Sciences, XXXVIII-1/(September)*, 167–171. https://doi.org/10.5194/isprsarchives-xxxviii-1-c22-167-2011

[41] Obaid, L., Hamad, K., Al-Ruzouq, R., Dabous, S. A., Ismail, K., & Alotaibi, E. (2025). State-of-the-art review of unmanned aerial vehicles (UAVs) and artificial intelligence (AI) for traffic and safety analyses: Recent progress, applications, challenges, and opportunities. *Transportation Research Interdisciplinary Perspectives, 33*, 101591. https://doi.org/https://doi.org/10.1016/j.trip.2025.101591

[42] Zolkepli, M. F., Ishak, M. F., Sidik, M. H., Ibrahim, N. A. S., & Zaini, M. S. I. (2021). Slope Mapping using Unmanned Aerial Vehicle (UAV). *Turkish Journal of Computer and Mathematics Education, 12(3)*, 1781–1789. https://doi.org/10.17762/turcomat.v12i3.1005

[43] Zhishui, L., Liu, H., Zhao, Y., Wang, Q., Wu, Z., Deng, L., & Gao, H. (2020). Effects of rainfall intensity, slope angle, and vegetation coverage on the erosion characteristics of Pisha sandstone slopes under simulated rainfall conditions. *Environmental Science and Pollution Research*, 27. https://doi.org/10.1007/s11356-019-05348-y

[44] Galloway, H. M., & Zachery, A. L. (2020). *Finding Slope*. Soil Science Society of America.

[45] Ishak, M. F., Zolkepli, M. F., & Muhammad, N. (2020). Effectiveness of Unmanned Aerial Vehicle (UAV) for Digital Slope Mapping. *International Journal of Engineering Technology and Sciences, 7(2)*, 119–136. https://doi.org/10.15282/ijets.7.2.2020.1010

[46] Zolkepli, M. F., Ishak, M. F., Yunus, M. Y. M., Zaini, M. S. I., Wahap, M. S., Yasin, A. M., Sidik, M. H., & Hezmi, M. A. (2021). Application of unmanned aerial vehicle (UAV) for slope mapping at Pahang Matriculation College, Malaysia. *Physics and Chemistry of the Earth, 123(February)*. https://doi.org/10.1016/j.pce.2021.103003

[47] Huat, L. T., & Ali, F. (2012). Slope hazard assessment in urbanized area. *Electronic Journal of Geotechnical Engineering, 17 C(February), 341–352*.